Nonlinear mixing of collective modes in harmonically trapped Bose-Einstein condensates

Takahiro Mizoguchi,* Shohei Watabe, and Tetsuro Nikuni
Tokyo University of Science, 1-3 Kagurazaka, Shinjuku-ku, Tokyo 162-9601, Japan
(Received 28 December 2016; published 21 March 2017)

We study nonlinear mixing effects among quadrupole modes and scissors modes in a harmonically trapped Bose-Einstein condensate. Using a perturbative technique in conjunction with a variational approach with a Gaussian trial wave function for the Gross-Pitaevskii equation, we find that mode mixing occurs selectively. Our perturbative approach is useful in gaining a qualitative understanding of the recent experiment [M. Yamazaki *et al.*, J. Phys. Soc. Jpn. **84**, 44001 (2015)], exhibiting a beating phenomenon of the scissors mode as well as a modulation phenomenon of the low-lying quadrupole mode by the high-lying quadrupole mode frequency. Within the second-order treatment of the nonlinear mode coupling terms, our approach predicts all the spectral peaks obtained by the numerical simulation of the Gross-Pitaevskii equation.

DOI: 10.1103/PhysRevA.95.033623

I. INTRODUCTION

Collective modes, such as dipole, quadrupole, and scissors modes, in harmonically trapped ultracold atomic gases have attracted much attention because they offer many-body physics as well as macroscopic quantum phenomena of Bose-Einstein condensates (BECs) [1–5]. In particular, the scissors mode in a BEC manifests superfluidity because of its irrotational nature [4–8]. Frequencies of the collective modes observed in the experiment [1] can be successfully described by the linearized Gross-Pitaevskii (GP) equation for the condensate at $T = 0$ [9,10]. Nonzero temperature effects [7,8,11] as well as the Beliaev process [12] are also important for explaining experimental results [3–5,12], which are not explained by linearized equations at $T = 0$ alone.

Even in the case at $T = 0$, however, we are faced with an important problem that is not explained by the linear analysis. Recently, various kinds of collective modes in a BEC—low-lying and high-lying quadrupole modes, as well as scissors modes—are simultaneously excited in a cigar-shaped trap [13]. This experiment has shown that oscillations of a scissors mode exhibits beating with a longer period oscillation, whose frequency is that of the low-lying quadrupole mode. The low-lying quadrupole mode is, on the other hand, modulated by a shorter period oscillation with the high-lying quadrupole mode frequency. Since these phenomena cannot be described by the linearized GP equation, we are confronted with the following questions: (i) Why does the scissors mode exhibit beating with the low-lying quadrupole mode frequency? (ii) Why is the low-lying quadrupole mode modulated by the high-lying quadrupole mode frequency? and (iii) How is a collective mode possibly modulated by the other collective mode frequencies in a trapped Bose gas? These phenomena may be seen widely, since a phenomenon similar to Ref. [13] has also been reported in a condensate response using a broadband probe with a wide range of frequencies [14], where spectra at several sum and difference frequencies are slightly visible.

Since these mode mixing effects are not included in the linear analysis, the phenomena we are interested in are beyond linear analysis. In this paper, we study these nonlinear effects of collective modes by using a perturbative approach in conjunction with a variational calculation with a Gaussian trial wave function [15]. We show that the perturbative study successfully explains the modulation phenomena of collective modes observed in the experiment in Ref. [13]. The mode mixing effects shown in Ref. [13] are concluded to be due to nonlinear effects. The nonlinear mixing weight $G'_{\rho\sigma\tau}$ obtained in this paper clearly shows that mode mixing occurs selectively, and these weights answer all three questions raised above. For the simultaneous excitation of quadrupole and scissors modes, by using a second-order perturbative treatment in the nonlinear-mode coupling terms, we successfully predict all spectral peaks obtained from the numerical simulation of the GP equation.

II. VARIATIONAL ANALYSIS

We derive nonlinear equations in order to understand nonlinear mixing of scissors and quadrupole modes. An earlier study [15] considered nonlinear coupling between scissors modes with different symmetries. In this section, we extend their variational analysis with a Gaussian trail wave function [15] to include mixing effects between both quadrupole and scissors modes in a trapped condensate.

As in Ref. [15], we start with the Lagrangian for the condensate order parameter $\psi(\mathbf{r},t)$, given by

$$L[\psi,\psi^*] = \frac{i\hbar}{2}\int d\mathbf{r}\left(\psi^*\frac{\partial\psi}{\partial t} - \psi\frac{\partial\psi^*}{\partial t}\right) - E[\psi,\psi^*], \quad (1)$$

where the energy functional is given by

$$E = \int d\mathbf{r}\left[\frac{\hbar^2}{2m}|\nabla\psi|^2 + V|\psi|^2 + \frac{g}{2}|\psi|^4 - \mu|\psi|^2\right]. \quad (2)$$

Here, $g = 4\pi a\hbar^2/m$ is a coupling constant, a the s-wave scattering length, and m the atomic mass. Its Euler-Lagrange equation is the GP equation

$$i\hbar\frac{\partial\psi(\mathbf{r},t)}{\partial t} = \left[-\frac{\hbar^2\nabla^2}{2m} + V(\mathbf{r}) + g|\psi(\mathbf{r},t)|^2\right]\psi(\mathbf{r},t). \quad (3)$$

*1214633@alumni.tus.ac.jp

The external trap potential is given by

$$V(\mathbf{r}) = \frac{m}{2}\left(\omega_x^2 x^2 + \omega_y^2 y^2 + \omega_z^2 z^2\right) = \frac{m}{2}\omega_\perp^2\left(\kappa^2 x^2 + y^2/\kappa^2 + \lambda^2 z^2\right), \tag{4}$$

where ω_x, ω_y, and ω_z are the trap frequencies in the x, y, and z directions, respectively. The parameters κ, λ, and $\omega_\perp$ are given by $\omega_\perp = \sqrt{\omega_x\omega_y}$, $\kappa = \omega_x/\omega_y$, and $\lambda = \omega_z/\sqrt{\omega_x\omega_y}$. In this section, we describe equations in terms of ω_x, ω_y, and ω_z to formulate general equations for arbitrary trap geometries. In the next section, we use the parameters $\omega_\perp$ and λ to study the axially symmetric trap case ($\kappa = 1$).

We introduce the following trial function for the condensate order parameter [15]:

$$\psi(\mathbf{r},t) = A(t)\exp[-b_x(t)x^2 - b_y(t)y^2 - b_z(t)z^2 - c_{xy}(t)xy - c_{yz}(t)yz - c_{zx}(t)zx], \tag{5}$$

where b_ζ and $c_{\zeta\eta}$ ($\zeta,\eta = x,y,z$) are complex variational parameters. The parameter A is a normalization factor to ensure the conservation of the total number of condensate atoms N, which is given by

$$A(t) = \frac{2^{1/4}\sqrt{N}}{\pi^{3/4}}\left[c_{xy,\mathrm{r}}c_{yz,\mathrm{r}}c_{zx,\mathrm{r}} + 4b_{x,\mathrm{r}}b_{y,\mathrm{r}}b_{z,\mathrm{r}} - \left(b_{z,\mathrm{r}}c_{xy,\mathrm{r}}^2 + b_{y,\mathrm{r}}c_{zx,\mathrm{r}}^2 + b_{x,\mathrm{r}}c_{yz,\mathrm{r}}^2\right)\right]^{1/4}, \tag{6}$$

where $b_{\zeta,\mathrm{r}}$ and $c_{\zeta\eta,\mathrm{r}}$ ($b_{\zeta,\mathrm{i}}$ and $c_{\zeta\eta,\mathrm{i}}$) are real (imaginary) parts of b_ζ and $c_{\zeta\eta}$, respectively.

We derive equations of motions for variational parameters for a BEC at $T = 0$ in three steps. First, by inserting the trial function, (5), into the Lagrangian, (1), and carrying out the spatial integration, we obtain

$$\begin{aligned}\frac{L[b,c]}{N} = {}& \frac{1}{Q}\left(\sum_{\zeta=x,y,z}\alpha_\zeta\dot{b}_{\zeta,\mathrm{i}} + \sum_{\{\zeta,\eta,\theta\}\in X}\beta_\zeta\dot{c}_{\eta\theta,\mathrm{i}}\right) \\ & - \frac{1}{2Q}\sum_{\{\zeta,\eta,\theta\}\in X}\alpha_\zeta(4|b_\zeta|^2 + |c_{\zeta\eta}|^2 + |c_{\theta\zeta}|^2) \\ & - \frac{1}{Q}\sum_{\{\zeta,\eta,\theta\}\in X}\sum_{\mathrm{p=r,i}}\beta_\zeta[2c_{\eta\theta,\mathrm{p}}(b_{\eta,\mathrm{p}} + b_{\theta,\mathrm{p}}) \\ & + c_{\zeta\eta,\mathrm{p}}c_{\theta\zeta,\mathrm{p}}] \\ & - \frac{1}{2Q}\sum_{\zeta=x,y,z}\alpha_\zeta\omega_\zeta^2 - \frac{\gamma}{2\sqrt{\pi}}\sqrt{Q},\end{aligned} \tag{7}$$

where $Q = 2\pi^3A^4/N$ and $\gamma = Na/L_{\mathrm{ho}}$. Here, $\alpha_\zeta \equiv 4b_{\eta,\mathrm{r}}b_{\theta,\mathrm{r}} - c_{\eta\theta,\mathrm{r}}^2$ and $\beta_\zeta \equiv c_{\theta\zeta,\mathrm{r}}c_{\zeta\eta,\mathrm{r}} - 2b_{\zeta,\mathrm{r}}c_{\eta\theta,\mathrm{r}}$, where the set $\{\zeta,\eta,\theta\}$ indicates Cartesian coordinates in cyclic order: $\{\zeta,\eta,\theta\} \in \{\{x,y,z\},\{y,z,x\},\{z,x,y\}\}$. An overdot represents a time derivative. All parameters have been scaled by the trap frequency $\bar{\omega} = (\omega_x\omega_y\omega_z)^{1/3}$ and the harmonic oscillator length $L_{\mathrm{ho}} = (\hbar/m\bar{\omega})$. The third term on the right-hand side of (7) was missing in the earlier study [15].

Second, we look for static equilibrium values of the variational parameters b_ζ^{equiv} and $c_{\zeta\eta}^{\mathrm{equiv}}$. Since the phase of the static order parameter ψ is uniform, we set $b_{\zeta,\mathrm{i}}^{\mathrm{equiv}} = c_{\zeta\eta,\mathrm{i}}^{\mathrm{equiv}} = 0$. Because of the symmetry of the trap potential, we can set $c_{\zeta\eta,\mathrm{r}}^{\mathrm{equiv}} = 0$. The equilibrium values of parameters b_ζ^{equiv} can be obtained by minimizing the energy functional, (2), which leads to

$$b_\zeta^{\mathrm{equiv}} = \left(\frac{\sqrt{\pi}}{8\gamma}\right)^{2/5}\omega_\zeta^2 \qquad (\zeta = x,y,z). \tag{8}$$

We then consider deviations of variational parameters $\delta b_\zeta(t) \equiv b_\zeta(t) - b_\zeta^{\mathrm{equiv}}$ and $\delta c_{\zeta\eta}(t) \equiv c_{\zeta\eta}(t) - c_{\zeta\eta}^{\mathrm{equiv}}$. It is useful to express these variational parameters in vector form:

$$\begin{aligned}\mathbf{p}^{\mathrm{T}} \equiv (&\delta b_{x,\mathrm{r}},\delta b_{y,\mathrm{r}},\delta b_{z,\mathrm{r}},\delta b_{x,\mathrm{i}},\delta b_{y,\mathrm{i}},\delta b_{z,\mathrm{i}}, \\ &\delta c_{xy,\mathrm{r}},\delta c_{yz,\mathrm{r}},\delta c_{zx,\mathrm{r}},\delta c_{xy,\mathrm{i}},\delta c_{yz,\mathrm{i}},\delta c_{zx,\mathrm{i}}).\end{aligned} \tag{9}$$

Finally, we expand the Lagrangian in terms of $\mathbf{p}$ and derive the Euler-Lagrange equations to second order in $\mathbf{p}$, which can be written in the form

$$iM_{\mu\nu}\dot{p}_\nu + F_{\mu\nu}p_\nu + G_{\mu\nu\xi}p_\nu p_\xi + H_{\mu\nu\xi}p_\nu\dot{p}_\xi = 0. \tag{10}$$

Here, p_ν is the νth component of the vector $\mathbf{p}$, and we use the Einstein summation convention, which implies taking the sum over the repeated indices. The coefficients $M_{\mu\nu}$ are pure imaginary, while $F_{\mu\nu}$, $G_{\mu\nu\xi}$, and $H_{\mu\nu\xi}$ are real. The coefficients $M_{\mu\nu}$, $F_{\mu\nu}$, and $G_{\mu\nu\xi}$ are (a)symmetrized such that $M_{\mu\nu} = -M_{\nu\mu}$, $F_{\mu\nu} = F_{\nu\mu}$, and $G_{\mu\nu\xi} = G_{\mu\xi\nu}$. Note that $H_{\mu\nu\xi}$ does not have symmetry. Matrix M is given by

$$M = i\pi^{1/5}\begin{pmatrix} 0 & M^{\mathrm{q}} & 0 & 0 \\ -M^{\mathrm{q}} & 0 & 0 & 0 \\ 0 & 0 & 0 & -M^{\mathrm{s}} \\ 0 & 0 & M^{\mathrm{s}} & 0 \end{pmatrix}, \tag{11}$$

where

$$M^{\mathrm{q}} = \mathrm{diag}\left(2\omega_y^4\omega_z^4,\ 2\omega_z^4\omega_x^4,\ 2\omega_x^4\omega_y^4\right), \tag{12}$$

$$M^{\mathrm{s}} = \mathrm{diag}\left(\omega_z^2,\ \omega_x^2,\ \omega_y^2\right), \tag{13}$$

and F is given by

$$F = \begin{pmatrix} F^{\mathrm{qr}} & 0 & 0 & 0 \\ 0 & F^{\mathrm{qi}} & 0 & 0 \\ 0 & 0 & F^{\mathrm{sr}} & 0 \\ 0 & 0 & 0 & F^{\mathrm{si}} \end{pmatrix}, \tag{14}$$

where

$$F^{\mathrm{qr}} = 2^{1/5}\gamma^{2/5}\begin{pmatrix} 3\omega_y^4\omega_z^4 & \omega_z^2 & \omega_y^2 \\ \omega_z^2 & 3\omega_z^4\omega_x^4 & \omega_x^2 \\ \omega_y^2 & \omega_x^2 & 3\omega_x^4\omega_y^4 \end{pmatrix}, \tag{15}$$

$$F^{\mathrm{qi}} = \frac{2^{9/5}}{\gamma^{2/5}}\mathrm{diag}\left(\omega_y^2\omega_z^2,\ \omega_z^2\omega_x^2,\ \omega_x^2\omega_y^2\right), \tag{16}$$

$$F^{\mathrm{sr}} = 2^{1/5}\gamma^{2/5}\mathrm{diag}\left(\omega_z^2,\ \omega_x^2,\ \omega_y^2\right), \tag{17}$$

$$F^{\mathrm{si}} = \frac{\pi^{2/5}}{2^{1/5}\gamma^{2/5}}\mathrm{diag}\left[\omega_z^2\left(\omega_x^2 + \omega_y^2\right),\ \omega_x^2\left(\omega_y^2 + \omega_z^2\right),\ \omega_y^2\left(\omega_z^2 + \omega_x^2\right)\right]. \tag{18}$$

III. PERTURBATIVE APPROACH

Within the linear approximation ignoring nonlinear terms that includes G and H in (10), we obtain the scissors

and quadrupole mode frequencies, which are consistent with those in the hydrodynamic (strongly interacting or large-N) limit [10,15]. Such a linear approximation is useful when we apply a single-frequency probe. However, if we excite collective modes simultaneously, nonlinear mode mixing may emerge and its effects are visible as in Refs. [13] and [14]. In order to study these effects beyond a linear analysis, we use the solution of a linear approximation as an unperturbed solution and regard the nonlinear terms as perturbation. To make this idea more concrete, we introduce a fictitious perturbation parameter ϵ such that

$$i M_{\mu\nu}\dot{p}_\nu + F_{\mu\nu}p_\nu + \epsilon(G_{\mu\nu\xi}p_\nu p_\xi + H_{\mu\nu\xi}p_\nu \dot{p}_\xi) = 0. \quad (19)$$

Following the usual perturbation technique, we set ϵ equal to unity at the end of the calculation. We look for an approximate solution as a power series of ϵ: $\mathbf{p} = \mathbf{p}^{(0)} + \epsilon\mathbf{p}^{(1)} + \epsilon^2\mathbf{p}^{(2)} + \ldots$. Substituting this power series into (19) and comparing the coefficients of each power of ϵ, we obtain a series of simultaneous equations.

The unperturbed equation, the zeroth order of ϵ, is given by

$$i M_{\mu\nu}\dot{p}_\nu^{(0)} + F_{\mu\nu}p_\nu^{(0)} = 0. \quad (20)$$

One can diagonalize this equation by a matrix S such that $\dot{q}_\rho^{(0)} = \mathrm{i}\Omega_\rho q_\rho^{(0)}$, where $p_\mu^{(0)} = S_{\mu\rho}q_\rho^{(0)}$ and Ω is a diagonal matrix given by $\Omega = S^{-1}M^{-1}FS$, whose elements are eigenvalues. The eigenvalues are real numbers, each two of them having the same absolute value with opposite sign. The solution $q_\rho^{(0)}$ can be given by $q_\rho^{(0)} = c_\rho^{(0)}\exp(\mathrm{i}\Omega_\rho t)$, where $c_\alpha^{(0)}$ determines the weights of eigenmodes under the initial condition.

In the following, we arrange eigenvalues such that

$$\Omega = \mathrm{diag}(-\Omega_{\mathrm{Q}}, \Omega_{\mathrm{Q}}, -\Omega_-, \Omega_-, -\Omega_+, \Omega_+, -\Omega_{xy}, \Omega_{xy}, -\Omega_{yz}, \Omega_{yz}, -\Omega_{zx}, \Omega_{zx}). \quad (21)$$

In an axially symmetric geometry ($\kappa = 1$), the frequencies $\Omega_{\mathrm{Q},\pm}$ correspond to the quadrupole mode frequencies, and the frequencies $\Omega_{xy,yz,zx}$ correspond to the scissors mode frequencies, which are given by

$$\begin{aligned}\Omega_{\mathrm{Q}}^2 &= \Omega_{xy}^2 = \frac{2}{\lambda^{2/3}},\\ \Omega_\pm^2 &= \frac{4+3\lambda^2 \pm \sqrt{16-16\lambda^2+9\lambda^4}}{2\lambda^{2/3}},\\ \Omega_{zx}^2 &= \Omega_{yz}^2 = \frac{1+\lambda^2}{\lambda^{2/3}}.\end{aligned} \quad (22)$$

The mode with $\Omega_{+(-)}$ is the high (low)-lying quadrupole-monopole excitation. In an axially symmetric trap, the Ω_{Q} quadrupole mode and the xy scissors mode degenerate, as do the yz scissors mode and the zx scissors mode. Figure 1 shows the λ dependence of these frequencies. These frequencies are consistent with those for a trapped condensate in the hydrodynamic limit [10].

Collecting terms of first order in ϵ, we obtain

$$i M_{\mu\nu}\dot{p}_\nu^{(1)} + F_{\mu\nu}p_\nu^{(1)} + f_\mu^{(0,0)} = 0, \quad (23)$$

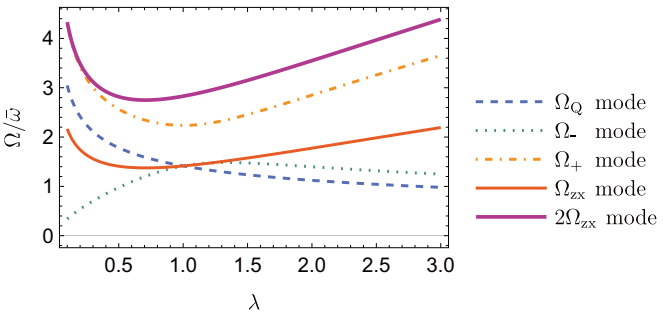

FIG. 1. The λ dependence of frequencies Ω_{Q}, $\Omega_\pm$, Ω_{zx} as well as $2\Omega_{zx}$ in an axially symmetric trap case ($\kappa = 1$). The frequencies Ω_{yz} and Ω_{xy} are equal to Ω_{zx} and Ω_{Q}, respectively.

where $f_\mu^{(i,j)} \equiv G_{\mu\nu\xi}p_\nu^{(i)}p_\xi^{(j)} + H_{\mu\nu\xi}p_\nu^{(i)}\dot{p}_\xi^{(j)}$. Using the transformation S, this equation reads as

$$\dot{q}_\rho^{(1)} = i\Omega_\rho q_\rho^{(1)} + iS_{\rho\nu'}^{-1}M_{\nu'\mu}^{-1}f_\mu^{(0,0)}, \quad (24)$$

where $p_\nu^{(1)} \equiv S_{\nu\rho}q_\rho^{(1)}$. The second term on the right-hand side, $iS_{\rho\nu'}^{-1}M_{\nu'\mu}^{-1}f_\mu^{(0,0)}$, represents nonlinear couplings between collective modes, i.e., the eigenmodes in the linearized equation (20). In order to clearly understand the nonlinear mixing effects of eigenmodes, it is more convenient to express the nonlinear term as $iS_{\rho\nu'}^{-1}M_{\nu'\mu}^{-1}f_\mu^{(0,0)} = G'_{\rho\sigma\tau}q_\sigma^{(0)}q_\tau^{(0)}$. From this expression, we find that the ρth mode is modulated by nonlinear mixing with the σth and τth modes through the term

$$G'_{\rho\sigma\tau}c_\sigma^{(0)}c_\tau^{(0)}\exp[i(\Omega_\sigma + \Omega_\tau)t]. \quad (25)$$

This shows that the ρth mode is modulated by an oscillation with frequency $\Omega_\sigma + \Omega_\tau$, where we represent this effect as $\rho \leftarrow \sigma + \tau$ or $\Omega_\rho \leftarrow \Omega_\sigma + \Omega_\tau$. Although the resultant nonlinear mixing may depend on the initial condition $c_\rho^{(0)}(\rho = 1,2,\ldots,12)$, the weight $G'_{\rho\sigma\tau}$ is quite important in understanding the nonlinear mixing between eigenmodes in (20), because it determines the presence or absence of nonlinear mixing. It is straightforward to find that the nonlinear mixing weight G' is given by

$$G'_{\rho\sigma\tau} \equiv iS_{\rho\nu'}^{-1}M_{\nu'\mu}^{-1}\Big[G_{\mu\nu\xi}S_{\nu\sigma}S_{\xi\tau} + \frac{i}{2}H_{\mu\nu\xi}(S_{\nu\sigma}S_{\xi\tau}\Omega_\tau + S_{\nu\tau}S_{\xi\sigma}\Omega_\sigma)\Big], \quad (26)$$

where G' is symmetric such that $G'_{\rho\sigma\tau} = G'_{\rho\tau\sigma}$.

Figure 2 shows the absolute values of the nonlinear mixing weight $G'_\rho(\rho = \text{even})$ in matrix form (column and row indices correspond to σ and τ, respectively) in a cigar-shaped trap case ($\lambda = 0.14$, which corresponds to the experiment in Ref. [13]). We do not show cases where ρ is odd, because we have the relation $G'_{\rho+1,\sigma+1,\tau+1} = (G'_{\rho\sigma\tau})^*$ for (ρ,σ,τ) odd, where this relation stems from the relation $q_{\rho+1}^{(1)} = (q_\rho^{(1)})^*$ for ρ odd. Some specific elements in matrices G'_ρ are absent, regardless of the value of the parameter λ, which indicates the absence of nonlinear mixing of collective modes, as well as the selectiveness of the nonlinear mixing.

Nonlinear mixing for the quadrupole modes is clearly distinct from that for the scissors modes. Matrices G'_2, G'_4,

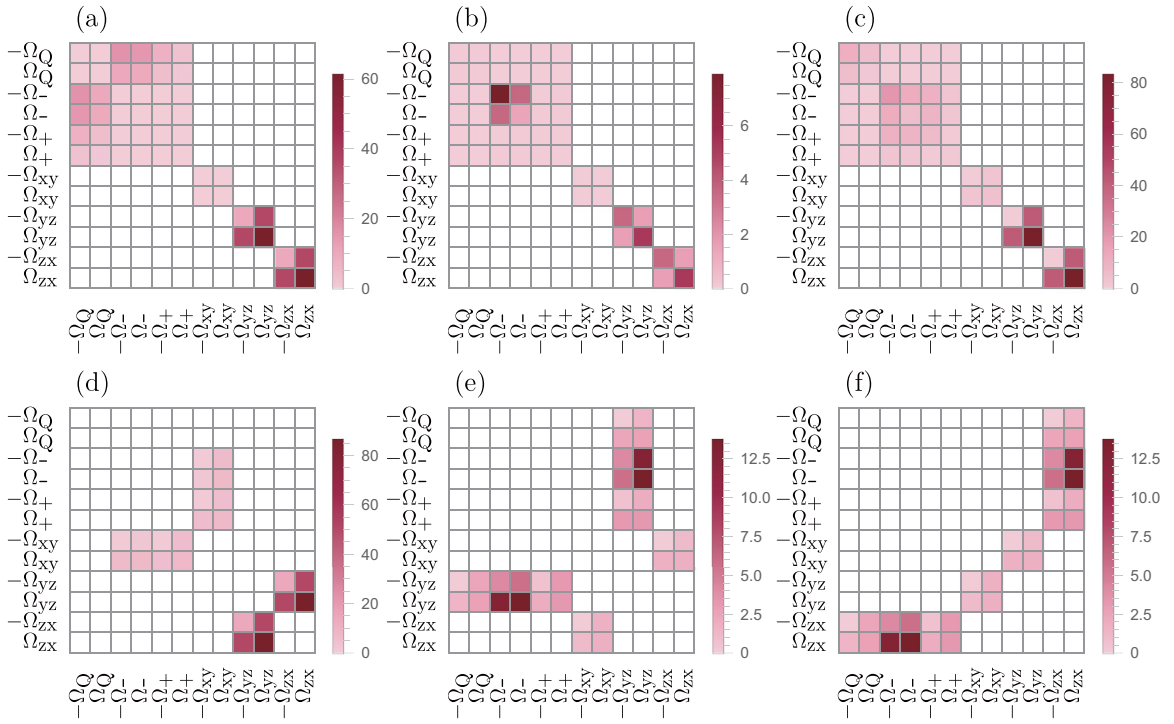

FIG. 2. Absolute values of the nonlinear mixing weight $G'_{\rho\sigma\tau}$ in the matrix form in a cigar-shaped trap case ($\lambda = 0.14$). (a) Matrix $G'_{2,\sigma,\tau}$(Ω_Q mode), (b) matrix $G'_{4,\sigma,\tau}$ (Ω_- mode), (c) matrix $G'_{6,\sigma,\tau}$ (Ω_+ mode), (d) matrix $G'_{8,\sigma,\tau}$ (Ω_{xy} mode), (e) matrix $G'_{10,\sigma,\tau}$ (Ω_{yz} mode), and (f) matrix $G'_{12,\sigma,\tau}$ (Ω_{zx} mode). The row and column of the matrix represent the σ and τ indices, respectively. The (σ,τ) section of each matrix provides the modulation term with the frequency $\Omega_\sigma + \Omega_\tau$ for the ρth mode. For instance, the $(\sigma = 1, \tau = 12)$ section of each matrix provides the modulation term with $\Omega_1 + \Omega_{12} = -\Omega_Q + \Omega_{zx}$. White elements are exactly 0 for arbitrary λ, where the nonlinear mixing is absent. The absolute value of $G'_{\rho\sigma\tau}$ is equal to that of $G'_{\rho+1,\sigma+1,\tau+1}$ when (ρ,σ,τ) are odd.

and G'_6, for three quadrupole modes which have essentially the same structure, have two characteristic features [Figs. 2(a), 2(b), and 2(c)]. First, all the quadrupole modes are coupled with each other, including themselves. This indicates that $\Omega_{Q,\pm} \leftarrow \Omega_{Q,\pm} \pm \Omega_{Q,\pm}$. Second, matrices G'_2, G'_4, and G'_6 involve a tridiagonal matrix, which leads to the nonlinear mixing $\Omega_{Q,\pm} \leftarrow \Omega_{xy,yz,zx} + \Omega_{xy,yz,zx}$. Others such as $\Omega_{Q,\pm} \leftarrow \Omega_{Q,\pm} \pm \Omega_{xy,yz,zx}$ and $\Omega_{Q,\pm} \leftarrow \Omega_{xy} \pm \Omega_{zx}$ do not occur.

Matrices G'_8, G'_{10}, and G'_{12} for the scissors modes have two distinct features [Figs. 2(d), 2(e), and 2(f)]. First, nonlinear mixing of all quadrupole modes ($\Omega_{xy,yz,zx} \leftarrow \Omega_{Q,\pm} \pm \Omega_{Q,\pm}$) is absent. Second, nonlinear mixing between a scissors mode and itself ($\sigma \leftarrow \sigma + \tau$ for $\sigma,\tau = 7,8,\ldots,12$) is also absent. These two features are in contrast with those for G'_2, G'_4, and G'_6.

On the other hand, a common feature can be found with respect to the beating phenomenon. From all the matrices, G'_2, G'_4, G'_6, G'_8, G'_{10}, and G'_{12}, we find that the beating effect is caused by the quadrupole modes. Indeed, for the σth mode, we have a nonlinear mixing term with $\sigma \leftarrow \sigma + \tau$ for $\Omega_\tau = \Omega_Q$ and $\Omega_\pm$, where an exception is for the scissors mode in the x-y plane, coupling with the quadrupole mode ($\Omega_\tau = \Omega_Q$) being absent.

The nonlinear mixing weight G' is helpful in understanding a recent experiment [13]. In this experiment, the zx scissors mode with frequency Ω_{zx} shows the beating phenomenon, where its oscillation amplitude is modulated by the longer-period oscillation with low-lying quadrupole mode frequency Ω_-. For the zx scissors mode, the matrix elements of $G'_{12,\sigma,\tau}$ for the $(\Omega_{zx}, \pm\Omega_-)$ sector are quite large compared with the other matrix elements [Fig. 2(f)]. This indicates that nonlinear mixing between the zx scissors mode (Ω_{zx}) and the low-lying quadrupole mode ($\pm\Omega_-$) is strong, and the beating emerges from the term $\exp[i(\Omega_{zx} \pm \Omega_-)t]$. This fact clearly explains the experimental results [13].

Our perturbative approach also answers the question why the oscillation of the low-lying quadrupole mode was modulated by the short-period oscillation with a high-lying quadrupole mode frequency (Ω_+). For the low-lying quadrupole mode (Ω_-), we find relatively large matrix elements in $G'_{4,\sigma,\tau}$ for the $(\Omega_{yz(zx)}, \Omega_{yz(zx)})$ sections [Fig. 2(b)]. This indicates that the low-lying quadrupole mode is modulated by the oscillation $\exp[i2\Omega_{yz(zx)}t]$. Since the high-lying quadrupole mode frequency satisfies $\Omega_+ \simeq 2\Omega_{yz(zx)}$ in the cigar-shaped trap case ($\lambda \ll 1$) (see Fig. 1), which is the case in the experiment in [13], the modulation of the low-lying quadrupole mode may be due to the nonlinear mixing between the $yz(zx)$ scissors modes, not due to the mixing between the low-lying and high-lying quadrupole modes. If the modulation were caused by the nonlinear mixing between these low-lying and high-lying quadrupole modes, the beating phenomenon could emerge as in the scissors mode case. However, this was not the case in the experiment in [13], where beating phenomena were not observed in the low-lying quadrupole mode. This result is supported by the fact that the matrix

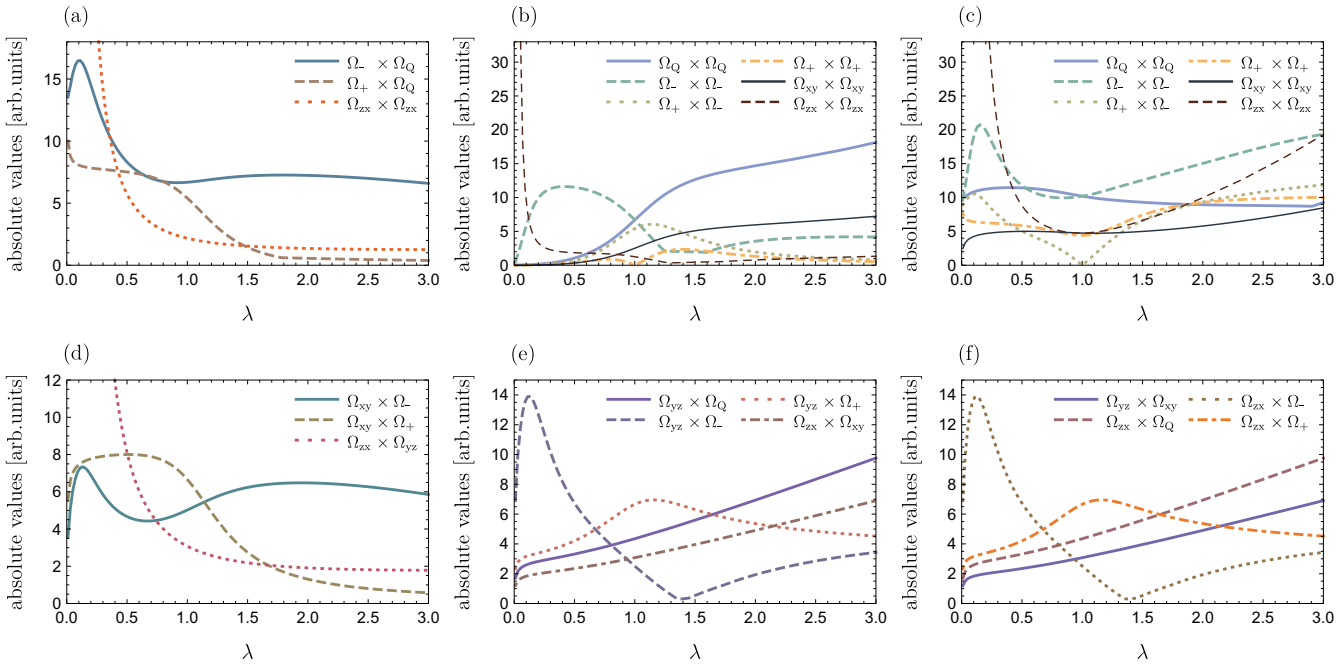

FIG. 3. The λ dependence of the mixing weight for (a) the Ω_Q mode, (b) the Ω_- mode, (c) the Ω_+ mode, (d) the Ω_{xy} mode, (e) the Ω_{yz} mode, and (f) the Ω_{zx} mode. Each line is the maximum absolute value among each four matrix elements in G' for the $(\pm\Omega_j, \pm\Omega_k)$ sections as well as the $(\pm\Omega_j, \mp\Omega_k)$ sections. Elements with a value smaller than those presented here are not shown. For instance, in (a), the line for $\Omega_- \times \Omega_Q$ is given by the maximum value among $|G'_{213}|$, $|G'_{214}|$, $|G'_{223}|$, and $|G'_{224}|$, which correspond to $\Omega_Q \leftarrow -\Omega_- - \Omega_Q$, $\Omega_Q \leftarrow -\Omega_- + \Omega_Q$, $\Omega_Q \leftarrow +\Omega_- - \Omega_Q$, and $\Omega_Q \leftarrow +\Omega_- + \Omega_Q$, respectively. In (a)–(c), lines for $\Omega_{yz} \times \Omega_{yz}$, which are not shown here, are the same as those for $\Omega_{zx} \times \Omega_{zx}$, because of an axially symmetric geometry case ($\kappa = 1$).

element in the (Ω_-,Ω_+) section is much smaller than that in the $(\Omega_{yz(zx)},\Omega_{yz(zx)})$ section [Fig. 2(b)].

Figure 3 shows the λ dependence of the dominant nonlinear mixing weight in G'. We plot the maximum absolute value among four matrix elements in the $(\pm\Omega_\sigma, \pm\Omega_\tau)$ sections as well as in the $(\pm\Omega_\sigma, \mp\Omega_\tau)$ sections. In the cigar-shaped trap case ($\lambda \ll 1$), the dominant nonlinear mixing for the quadrupole mode $\Omega_{Q,\pm}$ is the mixing between the zx scissors modes and themselves, leading to the frequency $2\Omega_{zx}$ [Figs. 3(a), 3(b), and 3(c)]. The dominant nonlinear mixing for the $yz(zx)$ scissors mode is the mixing between the $yz(zx)$ scissors mode and the low-lying quadrupole mode, leading to the frequency $\Omega_{yz(zx)} \pm \Omega_-$ [Figs. 3(e) and 3(f)]. This is consistent with the experimental result [13]. On the other hand, in the pancake-shaped trap case ($\lambda \gg 1$), the dominant nonlinear mixing for the Ω_Q quadrupole mode is the mixing between it and the low-lying quadrupole mode.

We can also discuss frequencies in the second-order perturbation by using the nonlinear mixing terms $G'_{\rho\sigma\tau}$. In the second order of ϵ, we have

$$i M_{\mu\nu} \dot{p}^{(2)}_\nu + F_{\mu\nu} p^{(2)}_\nu + f^{(0,1)}_\mu + f^{(1,0)}_\mu = 0. \qquad (27)$$

The inhomogeneous terms, $i S^{-1}_{\rho\nu'} M^{-1}_{\nu'\mu} f^{(i,j)}_\mu$ for $(i,j) = (1,0)$ and $(0,1)$, have the same form as in the first-order case, (24). In the case $(i,j) = (1,0)$, the nonlinear mixing is given by $G'^{(1,0)}_{\rho\sigma\tau} q^{(1)}_\sigma q^{(0)}_\tau$, where $G'^{(1,0)}_{\rho\sigma\tau}$ is the same as $G'_{\rho\sigma\tau}$ in (26). On the other hand, in the case where $(i,j) = (0,1)$, the nonlinear mixing is given by $G'^{(0,1)}_{\rho\sigma\tau} q^{(0)}_\sigma q^{(1)}_\tau$, where $G'^{(0,1)}_{\rho\sigma\tau}$ is defined by replacing the frequencies Ω_σ and Ω_τ in (26) with the frequencies $q^{(1)}_\sigma$ and $q^{(1)}_\tau$, respectively. Although the values of $G'^{(0,1)}_{\rho\sigma\tau}$ itself may change from those given in (26), the position of matrix elements that are 0, where nonlinear mixing is absent, does not change. This aspect is very useful in predicting the modulation frequency in the second-order perturbation. For instance, in Fig. 2(a) for matrix $G'_{2\sigma\tau}$, the index of the Ω_Q row may be replaced with $\Omega_Q + \Omega_-$, since we have the modulation $\Omega_Q \leftarrow \Omega_Q + \Omega_-$ in the first-order perturbation. In the second-order perturbation, the modulation of the oscillation for the Ω_Q quadrupole mode then has the frequency with $2\Omega_Q + \Omega_-$ and $\Omega_Q + 2\Omega_-$, i.e., the modulations $\Omega_Q \leftarrow (\Omega_Q + \Omega_-) + \Omega_Q$ and $\Omega_Q \leftarrow (\Omega_Q + \Omega_-) + \Omega_-$ occur. On the other hand, in the same-order perturbation for the Ω_Q quadrupole mode, the modulation with the frequency $2\Omega_- + \Omega_{zx}$, i.e., the modulation $\Omega_Q \leftarrow (\Omega_- + \Omega_{zx}) + \Omega_-$, may be absent, since in the first-order perturbation, the modulation $\Omega_Q \leftarrow \Omega_- + \Omega_{zx}$ does not exist [Fig. 2(a)].

IV. COMPARISON WITH SPECTRAL ANALYSIS

We compare the analytical results in the previous section with the numerical simulation of the GP equation. In this simulation, we simultaneously excite the quadrupole modes and the scissors mode using a perturbative external potential, $\delta V(\mathbf{r},t) = \theta(-t)(0.2x^2 + 0.25y^2 + 0.1zx)$, in dimensionless form, where $\theta(t)$ is the Heaviside step function. This type of perturbative potential was used in the experiment in Ref. [13] to excite three kinds of the quadrupole modes with $\Omega_{Q,\pm}$ and the zx scissors mode with Ω_{zx}.

To extract the spectra of each collective mode, we employ the following three steps. First, we calculate moments [6,7,16] from the condensate wave function $\Psi(\mathbf{r},t)$, where the GP equation was numerically solved by applying the method in Ref. [17]. These moments are defined as $\langle\chi\rangle \equiv \int d\mathbf{r}\chi|\Psi(\mathbf{r},t)|^2$, where $\chi = x^2$, y^2, z^2, xy, yz, and zx. From these quantities, we evaluate deviations from the time-averaged values. Second, we relate these moments to vector $\mathbf{p}$ in (9) within the linear approximation. One finds that the explicit relations are given by

$$\langle x^2\rangle \simeq -\left(\frac{2}{\pi}\right)^{2/5}\frac{\gamma^{4/5}}{\omega_x^4}\delta b_{x,\mathrm{r}}, \tag{28}$$

$$\langle x v_x\rangle \simeq \frac{2}{b_x^{(0)}}\delta b_{x,\mathrm{i}}, \tag{29}$$

$$\langle xy\rangle \simeq -\frac{\gamma^{4/5}}{2^{3/5}\pi^{2/5}\omega_x^2\omega_y^2}\delta c_{xy,\mathrm{r}}, \tag{30}$$

$$\langle x v_y + y v_x\rangle \simeq \left(\frac{1}{b_x^{(0)}}+\frac{1}{b_y^{(0)}}\right)\delta c_{xy,\mathrm{i}}. \tag{31}$$

The analogous relations for the other moments are easily obtained. These relations enable us to give vector $\mathbf{p}$ as a function of the moment $\langle\chi\rangle$, instead of the variational parameters δb_ν and $\delta c_{\mu\nu}$. Finally, we apply the Fourier transformation to the vector $\mathbf{q}(\langle\chi\rangle) \equiv S^{-1}\mathbf{p}(\langle\chi\rangle)$.

Figure 4 shows the spectral intensities obtained from the numerical simulation of the GP equation. All peaks are excellently explained by our perturbative approach within the second-order analysis (Fig. 4). One sees a relatively weak peak at the high-lying quadrupole mode frequency Ω_+ in the Ω_Q quadrupole mode [Fig. 4(a)]. This is because in order to extract each collective mode, we apply linear approximations such as (28) and (29) to $\langle\chi\rangle$, which include all the nonlinear effects. This is the case in Figs. 4(b) and 4(c).

In the comparison of our perturbation approach with the numerical simulation, we use renormalized frequencies Ω_i that are determined from the principal spectral peaks in Fig. 4. This is because the frequencies in (22) are rather consistent with the hydrodynamic (strongly interacting or large-N) limit, where the kinetic pressure energy is negligible [10], and it is not the case in this numerical simulation. In the Appendix, we show results where the frequencies given in (22) are used. In the intermediate regime (not in the hydrodynamic regime), it is difficult to apply analytic calculations, but the collective mode frequencies obtained in the experiment [1] are well described by the numerical calculation of the linearized equation [9]. Since the eigenmodes numerically obtained from the linearized equation in the intermediate regime [9] are smoothly connected to those in the hydrodynamic limit [10], our perturbative approach is applicable beyond the hydrodynamic limit if we take renormalized frequencies. This is the reason that our perturbative approach well predicts all the spectral peaks obtained in the numerical simulation beyond the hydrodynamic limit. The merit of our present approach using the nonlinear mixing weight is that it gives a clear physical understanding of nonlinear mixing effects between specific collective modes, such as quadrupole modes as well as scissors modes.

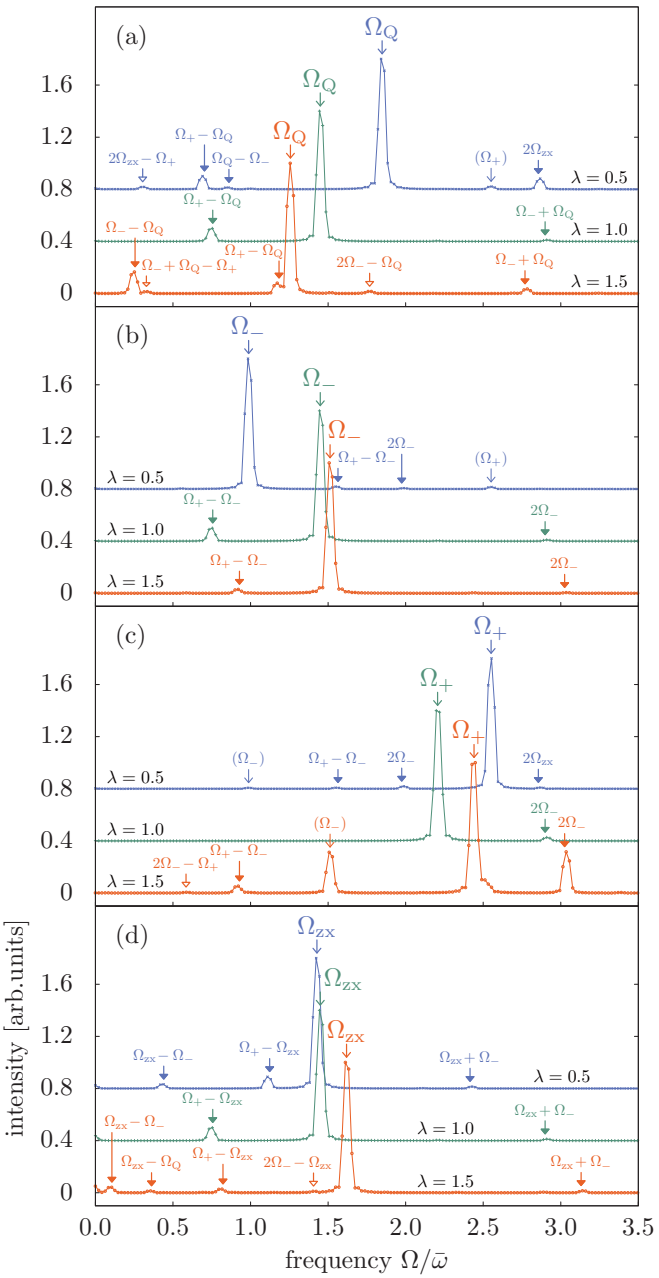

FIG. 4. Spectral intensities of (a) the Ω_Q mode, (b) the Ω_- mode, (c) the Ω_+ mode, and (d) the Ω_{zx} mode, obtained from numerical simulation of the GP equation in axially symmetric trap cases ($\lambda = 0.5, 1.0, 1.5$). Arrows with the largest labels in each panel indicate the frequencies $\Omega_{\mathrm{Q},\pm,zx}$ that are determined by the maximum peak position. Filled-head (open-head) arrows together with a linear combination of the Ω_i labels represent frequencies predicted by the first-order (second-order) perturbation approximation. (a–c) The spectrum of the quadrupole mode involves another quadrupole-mode peak, indicated by the arrow with the parenthetical label (Ω_i), because each collective mode is extracted from the linear approximations such as (28) and (29) by using moments $\langle x^2\rangle$, $\langle y^2\rangle$, and $\langle z^2\rangle$ obtained from the nonlinear numerical simulation.

V. CONCLUSION

To understand nonlinear mixing effects among collective modes in harmonically trapped Bose-Einstein condensates,

we studied quadrupole modes and scissors modes using a variational calculation with a Gaussian trial wave function together with a perturbation approach. We derived equations of motions for variational parameters to second order in fluctuations and applied a perturbative approach to reveal the structure of nonlinear couplings between unperturbed collective modes. We estimated the nonlinear mixing weight and found that mode mixing occurs selectively.

Although it is not always guaranteed to apply perturbative techniques to nonlinear equations, such as the Gross-Pitaevskii equation, our approach clearly explains the recent experiment [13] where the scissors mode exhibits the beating phenomenon with a longer-period oscillation that corresponds to the low-lying quadrupole mode frequency, and the oscillation of the low-lying quadrupole mode is modulated by a shorter-period oscillation with the high-lying quadrupole mode frequency. All the spectral peaks numerically obtained from the Gross-Pitaevskii equation are also excellently explained with the application of a second-order perturbation analysis, despite the case where the hydrodynamic limit approach is not applied. The nonlinear mixing weights obtained in our perturbation study will be helpful in understanding nonlinear mixing effects between collective modes in trapped Bose-Einstein condensates.

ACKNOWLEDGMENTS

The authors would like to thank M. Yamazaki for useful discussion. S.W. was partially supported by JSPS KAKENHI Grant No. JP16K17774.

APPENDIX

We show the results of a spectral analysis with the frequencies in (22) (Fig. 5). The situation for the numerical simulation is the same as that in Fig. 4. However, arrows are located based on the frequencies, (22), instead of the renormalized frequencies, Ω_i, determined from the frequencies giving maximum intensity peaks. In contrast to the case in Fig. 4, the arrows cannot well predict the peak positions of the spectra. This is because the frequencies in (22) obtained using the variational approach correspond to those in the hydrodynamic (strongly interacting or large-N) limit [15], which is not the case in the numerical simulation.

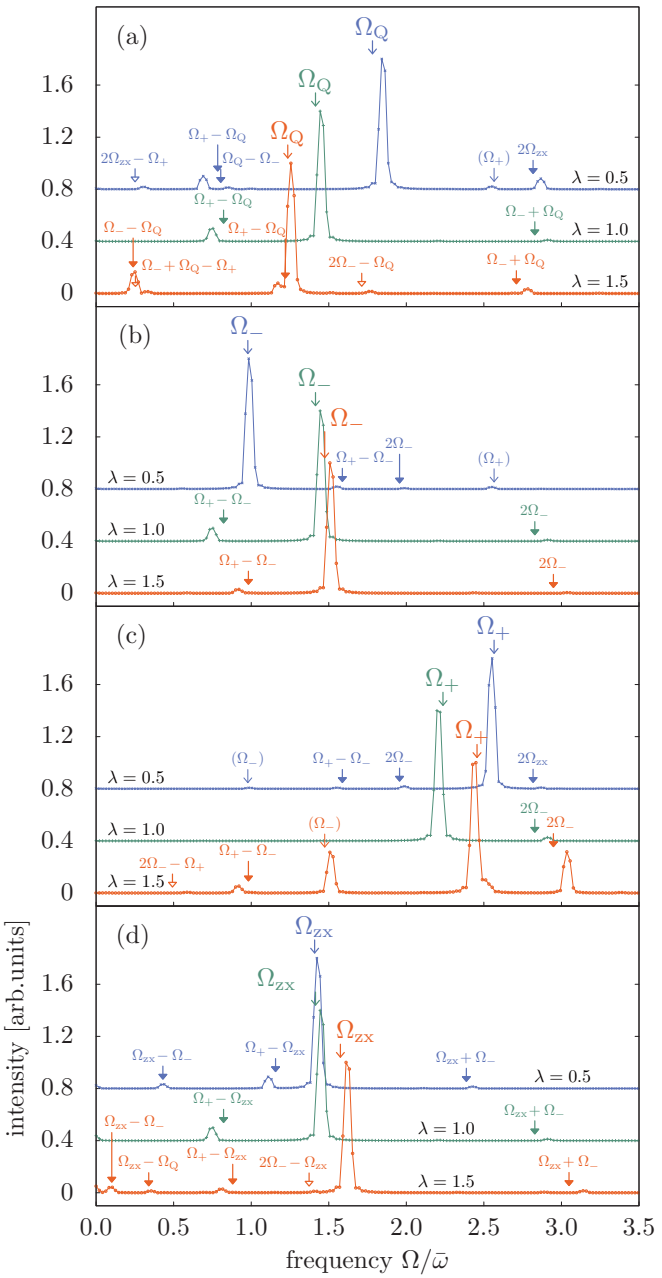

FIG. 5. Spectral intensities of modes for (a) the Ω_Q mode, (b) the Ω_- mode, (c) the Ω_+ mode, and (d) the Ω_{zx} mode, together with arrows pointing to the unperturbed frequencies, (22). The only difference between Fig. 4 and Fig. 5 is the use of renormalized frequencies vs unperturbed frequencies, (22), for arrows.

[1] D. S. Jin, J. R. Ensher, M. R. Matthews, C. E. Wieman, and E. A. Cornell, Phys. Rev. Lett. **77**, 420 (1996).

[2] M.-O. Mewes, M. R. Andrews, N. J. van Druten, D. M. Kurn, D. S. Durfee, C. G. Townsend, and W. Ketterle, Phys. Rev. Lett. **77**, 988 (1996).

[3] D. S. Jin, M. R. Matthews, J. R. Ensher, C. E. Wieman, and E. A. Cornell, Phys. Rev. Lett. **78**, 764 (1997).

[4] O. M. Maragò, S. A. Hopkins, J. Arlt, E. Hodby, G. Hechenblaikner, and C. J. Foot, Phys. Rev. Lett. **84**, 2056 (2000).

[5] O. Maragò, G. Hechenblaikner, E. Hodby, and C. Foot, Phys. Rev. Lett. **86**, 3938 (2001).

[6] D. Guéry-Odelin and S. Stringari, Phys. Rev. Lett. **83**, 4452 (1999).

[7] D. Guéry-Odelin, F. Zambelli, J. Dalibard, and S. Stringari, Phys. Rev. A **60**, 4851 (1999).

[8] B. Jackson and E. Zaremba, Phys. Rev. Lett. **87**, 100404 (2001).
[9] M. Edwards, P. A. Ruprecht, K. Burnett, R. J. Dodd, and C. W. Clark, Phys. Rev. Lett. **77**, 1671 (1996).
[10] S. Stringari, Phys. Rev. Lett. **77**, 2360 (1996).
[11] T. Nikuni, Phys. Rev. A **65**, 033611 (2002).
[12] E. Hodby, O. M. Maragò, G. Hechenblaikner, and C. J. Foot, Phys. Rev. Lett. **86**, 2196 (2001).
[13] M. Yamazaki, K. Wakayama, M. Harada, and A. Morinaga, J. Phys. Soc. Jpn. **84**, 44001 (2015).
[14] P. A. Ruprecht, M. Edwards, K. Burnett, and C. W. Clark, Phys. Rev. A **54**, 4178 (1996).
[15] U. Al Khawaja and H. T. C. Stoof, Phys. Rev. A **65**, 013605 (2001).
[16] A. Griffin, T. Nikuni, and E. Zaremba, *Bose-Condensed Gases at Finite Temperatures* (Cambridge University Press, Cambridge, UK, 2009).
[17] B. Jackson and E. Zaremba, Phys. Rev. A **66**, 033606 (2002).